

Analytic calculation of second-order electric response properties with the normalized elimination of the small component (NESC) method

Wenli Zou, Michael Filatov, and Dieter Cremer

Citation: *J. Chem. Phys.* **137**, 084108 (2012); doi: 10.1063/1.4747335

View online: <http://dx.doi.org/10.1063/1.4747335>

View Table of Contents: <http://jcp.aip.org/resource/1/JCPSA6/v137/i8>

Published by the [American Institute of Physics](#).

Additional information on *J. Chem. Phys.*

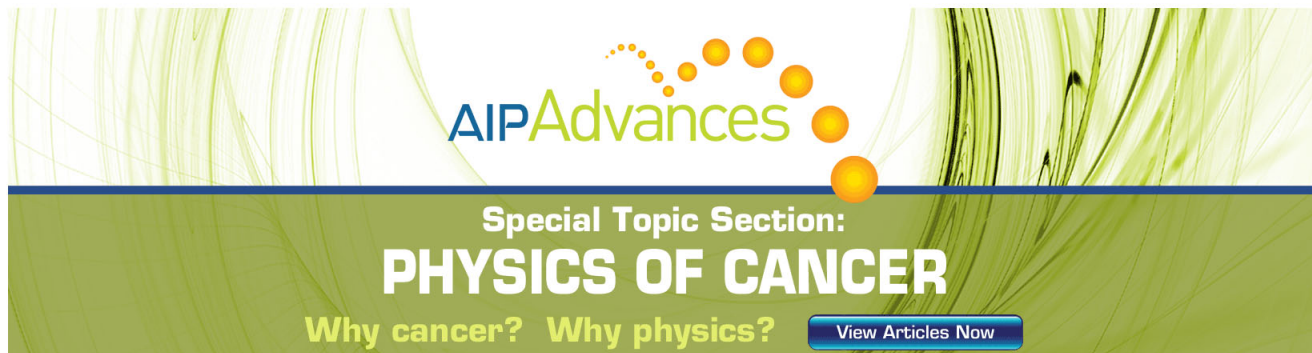
Journal Homepage: <http://jcp.aip.org/>

Journal Information: http://jcp.aip.org/about/about_the_journal

Top downloads: http://jcp.aip.org/features/most_downloaded

Information for Authors: <http://jcp.aip.org/authors>

ADVERTISEMENT



AIPAdvances

Special Topic Section:
PHYSICS OF CANCER

Why cancer? Why physics? [View Articles Now](#)

Analytic calculation of second-order electric response properties with the normalized elimination of the small component (NESC) method

Wenli Zou,¹ Michael Filatov,² and Dieter Cremer^{1,a)}

¹*Department of Chemistry, Southern Methodist University, 3215 Daniel Ave., Dallas, Texas 75275-0314, USA*

²*Mulliken Center for Theoretical Chemistry, Institut für Physikalische und Theoretische Chemie, Universität Bonn, Berlingstr. 4, D-53115 Bonn, Germany*

(Received 4 July 2012; accepted 6 August 2012; published online 28 August 2012)

Analytic second derivatives of the relativistic energy for the calculation of electric response properties are derived utilizing the normalized elimination of the small component (NESC) method. Explicit formulas are given for electric static dipole polarizabilities and infrared intensities by starting at the NESC representation of electric dipole moments. The analytic derivatives are implemented in an existing NESC program and applied to calculate dipole moments, polarizabilities, and the infrared spectra of gold- and mercury-containing molecules as well as some actinide molecules. Comparison with experiment reveals the accuracy of NESC second order electric response properties. © 2012 American Institute of Physics. [<http://dx.doi.org/10.1063/1.4747335>]

I. INTRODUCTION

The quantum chemical calculation of electric second order response properties with non-relativistic methods is a widely used standard procedure,¹ which is predominantly applied to organic molecules.² At the same time, there is less computational data available for molecules containing heavy elements because in this case, relativistic methods have to be applied.^{3–5} The complexity of the full four-component relativistic formalism restricts its applicability to atoms and small molecules^{6–9} and stimulates researchers to seek for simpler yet accurate computational alternatives. Here, we continue our method development work for the normalized elimination of the small component (NESC) method, which is an exact two-component relativistic method that was originally proposed by Dyall.¹⁰ In a series of previous publications, we developed and implemented a new algorithm for NESC,¹¹ which makes it possible to routinely carry out relativistic calculations for large molecules with heavy atoms. In addition, we worked out the methodology for calculating first order response properties,¹² such as the analytic energy gradient for geometry optimization, EPR hyperfine structure constants,¹³ contact densities for the calculation of Mössbauer isomer shifts,¹⁴ or electric field gradients for nuclear quadrupole coupling constants.¹⁵ In this work, we extend the previously developed formalism to the analytic calculation of electric second order response properties, such as polarizabilities and infrared (IR) intensities where our approach is based on the successful analytical calculation of NESC frequencies.¹⁶

When a molecule is exposed to an external electric field, the electric dipole moment measures the separation of positive and negative charge in the molecule whereas the static electric dipole polarizability measures the distortion of the molecular charge distribution.¹⁷ The polarizability is an important property that is essential for the understanding of the electronic structure. Knowledge of atomic and molecular polarizability

is important in many areas of computational chemistry ranging from electron and vibrational spectroscopy to molecular modeling, drug design, and nano-technology. In general, relativity leads to a contraction of the *s*- and *p*-orbitals and to an expansion of the *d*- and *f*-orbitals. In the case of atoms, the former effect (orbital contraction) dominates the charge distribution and leads to a reduction of the static electric polarizability. However, in molecules, the interplay between relativistic and electron correlation effects necessitates the use of accurate theoretical methods for explaining trends in a series of homologous compounds.¹⁸

The calculation of infrared (IR) intensities is even more important than the calculation of polarizabilities because the former are difficult to measure.¹⁹ Even in the year 2012, reliable absolute IR intensities are only known for small molecules in the gas phase. Most of the IR intensities measured are relative rather than absolute intensities. IR intensities provide valuable information about the charge distribution in a molecule under the impact of an external electromagnetic field.^{19,20}

In Secs. II–VIII, we will present first the NESC method (Sec. II), then the NESC dipole moment formulas (Sec. III), the formulas for the NESC polarizabilities (Sec. IV), and finally those for the NESC IR intensities (Sec. V). In Sec. VI, the computational procedures employed in this work will be described and calculated first and second order NESC properties obtained in this work will be discussed in Sec. VII. Conclusions will be drawn in Sec. VIII.

II. THE NESC METHOD

The NESC equation¹⁰ (1)

$$\tilde{\mathbf{L}}\mathbf{A} = \tilde{\mathbf{S}}\mathbf{A}\boldsymbol{\epsilon} \quad (1)$$

provides the exact electronic (positive-energy) solutions, i.e., eigenvectors \mathbf{A} and eigenvalues $\boldsymbol{\epsilon}$, of the one-electron Dirac equation.^{21,22} The NESC Hamiltonian $\tilde{\mathbf{L}}$ takes the form of

^{a)}Electronic mail: dcremer@gmail.com.

Eq. (2) (Refs. 10 and 11)

$$\tilde{\mathbf{L}} = \mathbf{U}^\dagger \mathbf{T} + \mathbf{T}\mathbf{U} + \mathbf{U}^\dagger (\mathbf{W} - \mathbf{T})\mathbf{U} + \mathbf{V}. \quad (2)$$

Here, \mathbf{S} , \mathbf{T} , and \mathbf{V} denote the matrices of the overlap, kinetic energy, and potential energy operators, and \mathbf{W} is the matrix of the operator $(\boldsymbol{\sigma} \cdot \mathbf{p})V(\mathbf{r})(\boldsymbol{\sigma} \cdot \mathbf{p})/4 \text{ m}^2\text{c}^2$ ($\nabla V(\mathbf{r}) \cdot \nabla/4 \text{ m}^2\text{c}^2$ in scalar relativistic approximation) in the basis of the atomic orbitals $\chi_\mu(\mathbf{r})$.¹⁰ The relativistic metric is given by Eq. (3).

$$\tilde{\mathbf{S}} = \mathbf{S} + \frac{1}{2\text{m}c^2} \mathbf{U}^\dagger \mathbf{T}\mathbf{U}. \quad (3)$$

Matrix \mathbf{U} connects the large component and the pseudo-large component of the electronic solutions of Dyll's modified 4-component Dirac equation,¹⁰ which can be calculated iteratively using one of the following equations:^{11,23–25}

$$\mathbf{U} = \mathbf{T}^{-1}(\mathbf{S}\tilde{\mathbf{S}}^{-1}\tilde{\mathbf{L}} - \mathbf{V}) \quad (4)$$

$$= (\mathbf{T} - \mathbf{W})^{-1} \mathbf{T} \left[\mathbf{I} - \frac{1}{2\text{m}c^2} \mathbf{U}\mathbf{S}^{-1}(\mathbf{T}\mathbf{U} + \mathbf{V}) \right], \quad (5)$$

or using the one-step method described by Zou and co-workers.¹¹ In the following, all derivations are taken in the scalar relativistic form.

In the case of a many-electron problem, the one-electron NESC Hamiltonian $\tilde{\mathbf{L}}$ has to be renormalized on the non-relativistic metric^{10,26}

$$\mathbf{H}_{1-e} = \mathbf{G}^\dagger \tilde{\mathbf{L}}\mathbf{G}, \quad (6)$$

where \mathbf{G} is the renormalization matrix,²⁷

$$\mathbf{G} = \mathbf{S}^{-1/2}(\mathbf{S}^{-1/2}\tilde{\mathbf{S}}\mathbf{S}^{-1/2})^{-1/2}\mathbf{S}^{1/2}, \quad (7)$$

implying that

$$\mathbf{G}\mathbf{G} = \tilde{\mathbf{S}}^{-1}\mathbf{S}. \quad (8)$$

For a closed-shell system, the Fock matrix is given by

$$\mathbf{F} = \mathbf{H}_{1-e} + (2\mathbf{J} - \mathbf{K}), \quad (9)$$

and the total electronic energy E of the many-electron system by Eq. (10),

$$E = \text{tr}\mathbf{P}\mathbf{H}_{1-e} + \frac{1}{2}\text{tr}\mathbf{P}(\mathbf{J} - \mathbf{K}), \quad (10)$$

where \mathbf{J} and \mathbf{K} are the Coulomb and exchange parts of the Fock matrix and \mathbf{P} is the density matrix calculated as $\mathbf{P} = \mathbf{C}\mathbf{n}\mathbf{C}^\dagger$. The diagonal matrix \mathbf{n} contains the orbital occupation numbers and matrix \mathbf{C} collects the eigenvectors of the Fock matrix obtained from the diagonalization of the pseudo-eigenvalue problem of Eq. (11)

$$\mathbf{F}\mathbf{C} = \mathbf{S}\mathbf{C}\epsilon. \quad (11)$$

In the following, the first and second derivatives of Eq. (10) are derived, which are needed for the analytic calculation of electric response properties.

III. DERIVATION OF THE NESC DIPOLE MOMENT

In a static homogeneous electric field \mathbf{F} , the potential $V(\mathbf{r})$ modifies to

$$V(\mathbf{r}) = V(\mathbf{F} = \mathbf{0}) + \mathbf{F} \cdot \mathbf{r}, \quad (12)$$

and the total molecular energy can be represented by a Taylor expansion as in

$$E(\mathbf{F}) = E(0) + \left. \frac{\partial E(\mathbf{F})}{\partial \mathbf{F}} \right|_{\mathbf{F}=\mathbf{0}} \cdot \mathbf{F} \quad (13)$$

$$+ \frac{1}{2} \mathbf{F} \cdot \left. \frac{\partial^2 E(\mathbf{F})}{\partial \mathbf{F} \partial \mathbf{F}} \right|_{\mathbf{F}=\mathbf{0}} \cdot \mathbf{F} + \dots \quad (14)$$

The first order term of the expansion leads to the electric dipole moment

$$\boldsymbol{\mu} = - \left. \frac{\partial E(\mathbf{F})}{\partial \mathbf{F}} \right|_{\mathbf{F}=\mathbf{0}}, \quad (15)$$

whereas the second order term gives the polarizability tensor

$$\boldsymbol{\alpha} = - \left. \frac{\partial^2 E(\mathbf{F})}{\partial \mathbf{F} \partial \mathbf{F}} \right|_{\mathbf{F}=\mathbf{0}}. \quad (16)$$

For convenience, one defines the scalar dipole moment as the norm of the dipole moment vector $\mu = \|\boldsymbol{\mu}\|$ and the isotropic polarizability as the average of the trace of the polarizability tensor

$$\bar{\alpha} = \frac{1}{3}(\alpha_{xx} + \alpha_{yy} + \alpha_{zz}), \quad (17)$$

which is invariant with regard to coordinate transformations.

Taking the derivative of the electronic energy (10) with regard to the components F_α ($\alpha = x, y, z$) of the electric field, only the terms depending on \mathbf{V} , \mathbf{W} , \mathbf{G} , and \mathbf{U} (since \mathbf{G} depends on \mathbf{U} , and \mathbf{U} depends on \mathbf{V} and \mathbf{W}), make contributions to the dipole moment component μ_α

$$\begin{aligned} \mu_\alpha &= -\text{tr}\mathbf{P} \frac{\partial \mathbf{H}_{1-e}}{\partial F_\alpha} = \text{tr} \left[\mathbf{P} \frac{\partial}{\partial F_\alpha} (\mathbf{G}^\dagger \tilde{\mathbf{L}}\mathbf{G}) \right] \\ &= -\text{tr}\tilde{\mathbf{P}} \frac{\partial \tilde{\mathbf{L}}}{\partial F_\alpha} + \text{tr} \left(\mathbf{D} \frac{\partial \mathbf{G}^\dagger}{\partial F_\alpha} + \mathbf{D}^\dagger \frac{\partial \mathbf{G}}{\partial F_\alpha} \right), \end{aligned} \quad (18)$$

where the new matrices $\tilde{\mathbf{P}} = \mathbf{G}\mathbf{P}\mathbf{G}^\dagger$ and $\mathbf{D} = \tilde{\mathbf{L}}\mathbf{G}\mathbf{P}$ are introduced.

The terms containing the $\partial \mathbf{W}/\partial F_\alpha$ and $\partial \mathbf{U}/\partial F_\alpha$ derivatives make only negligible contributions to the dipole moment. Indeed, the elements of the $\partial \mathbf{W}/\partial F_\alpha$ matrix depend on the gradient of the basis set functions χ_μ , which are large only in the core region, and are typically 3–4 orders of magnitude smaller than the dipole moment integrals $\partial \mathbf{V}/\partial F_\alpha = \langle \chi_\mu | \mathbf{r} | \chi_\nu \rangle$ in the valence region.²⁸ As follows from Eq. (5), the derivatives $\partial \mathbf{U}/\partial F_\alpha$ are of the order of $o(c^{-2})$ as compared to the dipole moment integrals and can be safely neglected.

The derivative of \mathbf{G} can be obtained by differentiating Eq. (8), which leads to Eq. (19),

$$\begin{aligned} \mathbf{G}\mathbf{X} + \mathbf{X}\mathbf{G} &= -\tilde{\mathbf{S}}^{-1} \frac{\partial \tilde{\mathbf{S}}}{\partial F_\alpha} \mathbf{G}\mathbf{G} = -\tilde{\mathbf{S}}^{-1} \left[\left(\frac{1}{2\text{m}c^2} \frac{\partial \mathbf{U}^\dagger}{\partial F_\alpha} \right) \mathbf{T}\mathbf{U} \right. \\ &\quad \left. + \mathbf{U}^\dagger \mathbf{T} \left(\frac{1}{2\text{m}c^2} \frac{\partial \mathbf{U}}{\partial F_\alpha} \right) \right] \mathbf{G}\mathbf{G}, \end{aligned} \quad (19)$$

where $\mathbf{X} = \partial \mathbf{G}/\partial F_\alpha$. Equation (19) can be solved by iteration or eigenvalue decomposition methods.¹⁶ However, $\partial \mathbf{G}/\partial F_\alpha$ is of the order $O(c^{-4})$ and therefore it can be also neglected.

In view of these considerations, Eq. (18) can be simplified to

$$\mu_\alpha = -tr\tilde{\mathbf{P}}\frac{\partial\tilde{\mathbf{L}}}{\partial F_\alpha} = -tr\tilde{\mathbf{P}}\frac{\partial\mathbf{V}}{\partial F_\alpha}. \quad (20)$$

This means that the dipole moment is calculated using the same formula as in the non-relativistic case except that the transformed density matrix $\tilde{\mathbf{P}}$ has to be used in the scalar relativistic case.

IV. DERIVATION OF THE NESC POLARIZABILITY

Taking the derivative of Eq. (18) with respect to F_β ($\alpha, \beta = x, y, z$), one obtains Eq. (21) for the polarizability tensor.

$$\begin{aligned} \alpha_{\alpha\beta} &= -\frac{\partial^2 E}{\partial F_\alpha \partial F_\beta} = \frac{\partial\mu_\alpha}{\partial F_\beta} \\ &= -tr\frac{\partial\mathbf{P}}{\partial F_\beta}\left(\frac{\partial\mathbf{G}^\dagger}{\partial F_\alpha}\tilde{\mathbf{L}}\mathbf{G} + \mathbf{G}^\dagger\frac{\partial\tilde{\mathbf{L}}}{\partial F_\alpha}\mathbf{G} + \mathbf{G}^\dagger\tilde{\mathbf{L}}\frac{\partial\mathbf{G}}{\partial F_\alpha}\right) \\ &\quad -tr\tilde{\mathbf{P}}\frac{\partial^2\tilde{\mathbf{L}}}{\partial F_\alpha\partial F_\beta} -tr\left(\mathbf{D}\frac{\partial^2\mathbf{G}^\dagger}{\partial F_\alpha\partial F_\beta} + \mathbf{D}^\dagger\frac{\partial^2\mathbf{G}}{\partial F_\alpha\partial F_\beta}\right) \\ &\quad -tr\mathbf{P}\left(\frac{\partial\mathbf{G}^\dagger}{\partial F_\alpha}\tilde{\mathbf{L}}\frac{\partial\mathbf{G}}{\partial F_\beta} + \frac{\partial\mathbf{G}^\dagger}{\partial F_\beta}\tilde{\mathbf{L}}\frac{\partial\mathbf{G}}{\partial F_\alpha}\right) -tr\mathbf{P}\left(\frac{\partial\mathbf{G}^\dagger}{\partial F_\alpha}\frac{\partial\tilde{\mathbf{L}}}{\partial F_\beta}\mathbf{G} \right. \\ &\quad \left. + \mathbf{G}^\dagger\frac{\partial\tilde{\mathbf{L}}}{\partial F_\beta}\frac{\partial\mathbf{G}}{\partial F_\alpha} + \frac{\partial\mathbf{G}^\dagger}{\partial F_\beta}\frac{\partial\tilde{\mathbf{L}}}{\partial F_\alpha}\mathbf{G} + \mathbf{G}^\dagger\frac{\partial\tilde{\mathbf{L}}}{\partial F_\alpha}\frac{\partial\mathbf{G}}{\partial F_\beta}\right). \quad (21) \end{aligned}$$

Similar to the case of the dipole moment, both the first and second derivatives of \mathbf{W} , \mathbf{U} , and \mathbf{G} can be neglected and in this way Eq. (21) simplifies to

$$\begin{aligned} \alpha_{\alpha\beta} &= -tr\tilde{\mathbf{P}}\frac{\partial^2\tilde{\mathbf{L}}}{\partial F_\alpha\partial F_\beta} -tr\frac{\partial\mathbf{P}}{\partial F_\alpha}\left(\mathbf{G}^\dagger\frac{\partial\tilde{\mathbf{L}}}{\partial F_\beta}\mathbf{G}\right) \\ &= -tr\tilde{\mathbf{P}}\frac{\partial^2\mathbf{V}}{\partial F_\alpha\partial F_\beta} -tr\frac{\partial\mathbf{P}}{\partial F_\alpha}\left(\mathbf{G}^\dagger\frac{\partial\mathbf{V}}{\partial F_\beta}\mathbf{G}\right). \quad (22) \end{aligned}$$

Since \mathbf{V} is a linear function of the external electric field, Eq. (12), the second derivative of \mathbf{V} in the first term on the rhs vanishes and Eq. (21) is further simplified to Eq. (23)

$$\alpha_{\alpha\beta} = -tr\frac{\partial\mathbf{P}}{\partial F_\alpha}\left(\mathbf{G}^\dagger\frac{\partial\mathbf{V}}{\partial F_\beta}\mathbf{G}\right). \quad (23)$$

Hence, the scalar relativistic formula for the polarizability differs from the non-relativistic calculation only by the fact that the derivative $\partial\mathbf{V}/\partial F_\beta$ has to be renormalized by matrix \mathbf{G} . The derivative of \mathbf{P} has to be calculated with the help of a coupled-perturbed (CP) approach.

V. DERIVATION OF THE NESC INFRARED INTENSITIES

The IR intensity is given by Eq. (24)

$$\Gamma_i = (8\pi^3 N_A g / 3hc) \left| \frac{\partial\boldsymbol{\mu}}{\partial Q_i} \right|^2, \quad (24)$$

where N_A is the Avogadro number, h the Planck constant, c the speed of light, Q_i the normal coordinate and g the degeneracy of normal mode \mathbf{d}_i for $i = 1, \dots, 3N - L = N_{vib}$ with

N being the number of atoms in a molecule and L the number of its translations and rotations. Since we calculate dipole moment derivatives for Cartesian coordinates $X = \{x, y, z\}$ and work in atomic units, the intensity of mode i can be rewritten as

$$\Gamma_i = \boldsymbol{\delta}_i^\dagger \boldsymbol{\delta}_i = \mathbf{I}_i^\dagger (\Delta^\dagger \Delta) \mathbf{I}_i, \quad (25)$$

$$\boldsymbol{\delta}_i = \Delta \mathbf{I}_i, \quad (26)$$

where Δ is the rectangular dipole moment derivative matrix of dimension $3 \times 3N$ given in Cartesian coordinates. By solving the vibrational secular equation in Cartesian coordinates, the normal vibrational modes \mathbf{I}_i are obtained. In Eq. (25), it is used that intensities expressed with regard to normal coordinates are related to those expressed in Cartesian coordinates by the equation

$$(\Delta^\mathcal{Q})^\dagger \Delta^\mathcal{Q} = \mathbf{I}_i^\dagger ((\Delta^X)^\dagger \Delta^X) \mathbf{I}_i. \quad (27)$$

IR intensities Γ_i are second order response properties because one has to take the first derivatives of the energy E with regard to the components of the electric field \mathbf{F} and then the second derivatives with regard to the Cartesian coordinates X_n ($n = 1, \dots, 3N$). For practical reasons, it is of advantage to revert the order of derivations and to calculate scalar relativistic NESC IR intensities utilizing the following formulas.

Taking the derivative of Eq. (18) with respect to an atomic coordinate X_n , one gets

$$\begin{aligned} \Delta_{\alpha,n} &= \frac{\partial^2 E}{\partial X_n \partial F_\alpha} = tr\frac{\partial\mathbf{P}}{\partial X_n}\frac{\partial\mathbf{H}_{1-e}}{\partial F_\alpha} + tr\mathbf{P}\frac{\partial^2\mathbf{H}_{1-e}}{\partial X_n \partial F_\alpha} \\ &= tr\frac{\partial\mathbf{P}}{\partial X_n}\left(\frac{\partial\mathbf{G}^\dagger}{\partial F_\alpha}\tilde{\mathbf{L}}\mathbf{G} + \mathbf{G}^\dagger\frac{\partial\tilde{\mathbf{L}}}{\partial F_\alpha}\mathbf{G} + \mathbf{G}^\dagger\tilde{\mathbf{L}}\frac{\partial\mathbf{G}}{\partial F_\alpha}\right) \\ &\quad + tr\tilde{\mathbf{P}}\frac{\partial^2\tilde{\mathbf{L}}}{\partial X_n \partial F_\alpha} + tr\left(\mathbf{D}\frac{\partial^2\mathbf{G}^\dagger}{\partial X_n \partial F_\alpha} + \mathbf{D}^\dagger\frac{\partial^2\mathbf{G}}{\partial X_n \partial F_\alpha}\right) \\ &\quad + tr\mathbf{P}\left(\frac{\partial\mathbf{G}^\dagger}{\partial X_n}\tilde{\mathbf{L}}\frac{\partial\mathbf{G}}{\partial F_\alpha} + \frac{\partial\mathbf{G}^\dagger}{\partial F_\alpha}\tilde{\mathbf{L}}\frac{\partial\mathbf{G}}{\partial X_n}\right) + tr\mathbf{P}\left(\frac{\partial\mathbf{G}^\dagger}{\partial X_n}\frac{\partial\tilde{\mathbf{L}}}{\partial F_\alpha}\mathbf{G} \right. \\ &\quad \left. + \mathbf{G}^\dagger\frac{\partial\tilde{\mathbf{L}}}{\partial F_\alpha}\frac{\partial\mathbf{G}}{\partial X_n} + \frac{\partial\mathbf{G}^\dagger}{\partial F_\alpha}\frac{\partial\tilde{\mathbf{L}}}{\partial X_n}\mathbf{G} + \mathbf{G}^\dagger\frac{\partial\tilde{\mathbf{L}}}{\partial X_n}\frac{\partial\mathbf{G}}{\partial F_\alpha}\right). \quad (28) \end{aligned}$$

Again, both the first and second derivatives of \mathbf{W} , \mathbf{U} , and \mathbf{G} are neglected, which leads to Eq. (29)

$$\begin{aligned} \Delta_{\alpha,n} &= tr\left(\tilde{\mathbf{P}}\frac{\partial^2\tilde{\mathbf{L}}}{\partial X_n \partial F_\alpha}\right) + tr\frac{\partial\mathbf{P}}{\partial X_n}\left(\mathbf{G}^\dagger\frac{\partial\tilde{\mathbf{L}}}{\partial F_\alpha}\mathbf{G}\right) \\ &= tr\left(\tilde{\mathbf{P}}\frac{\partial^2\mathbf{V}}{\partial X_n \partial F_\alpha}\right) + tr\frac{\partial\mathbf{P}}{\partial X_n}\left(\mathbf{G}^\dagger\frac{\partial\mathbf{V}}{\partial F_\alpha}\mathbf{G}\right). \quad (29) \end{aligned}$$

Alternatively, one can take the derivatives of Eq. (10) first with respect to X_n and then F_α to obtain Eq. (30),

$$\begin{aligned} \Delta_{n,\alpha} &= \frac{\partial^2 E}{\partial F_\alpha \partial X_n} = tr\mathbf{P}\frac{\partial^2\mathbf{H}_{1-e}}{\partial F_\alpha \partial X_n} + tr\frac{\partial\boldsymbol{\Omega}}{\partial F_\alpha}\frac{\partial\mathbf{S}}{\partial X_n} \\ &\quad + tr\frac{\partial\mathbf{P}}{\partial F_\alpha}\frac{\partial\mathbf{H}_{1-e}}{\partial X_n} + \frac{1}{2}tr\frac{\partial\mathbf{P}}{\partial F_\alpha}\frac{\partial'}{\partial X_n}(\mathbf{J} - \mathbf{K}), \quad (30) \end{aligned}$$

where matrix $\boldsymbol{\Omega}$ is defined by $\boldsymbol{\Omega} = -\mathbf{C}\boldsymbol{\epsilon}\mathbf{N}\mathbf{C}^\dagger$. After neglecting the first and second derivatives of \mathbf{W} , \mathbf{U} , and \mathbf{G} (and also

the ones of \mathbf{S} and \mathbf{T} since they are 3–4 orders of magnitude smaller than those of \mathbf{V}), Eq. (30) takes the form

$$\Delta_{n,\alpha} = \text{tr} \left(\tilde{\mathbf{P}} \frac{\partial^2 \mathbf{V}}{\partial X_n \partial F_\alpha} \right) + \text{tr} \frac{\partial \mathbf{P}}{\partial F_\alpha} \left(\mathbf{G}^\dagger \frac{\partial \mathbf{V}}{\partial X_n} \mathbf{G} \right) + \text{tr} \frac{\partial \Omega}{\partial F_\alpha} \frac{\partial \mathbf{S}}{\partial X_n} + \frac{1}{2} \text{tr} \frac{\partial \mathbf{P}}{\partial F_\alpha} \frac{\partial'}{\partial X_n} (\mathbf{J} - \mathbf{K}). \quad (31)$$

In comparison to Eq. (29), there are fewer CP equations to be solved in Eq. (31) (6 vs. $3N$), however more matrix multiplications ($27N$ vs. $9N$) have to be carried out. Also, the $\partial \mathbf{P} / \partial X_n$ derivatives can be obtained during the calculation of the vibrational frequencies¹⁶ and saved for further use in Eq. (29).

VI. COMPUTATIONAL PROCEDURES

The equations for NESC second order response properties described in Secs. II–V were implemented in the program COLOGNE12 (Ref. 29) and tested with the help of the IORamm (Infinite Order Regular Approximation with modified metric) program previously written by Filatov and Cremer.^{28,30}

The NESC second order response property program was applied to a series of molecules containing heavy and super-heavy atoms utilizing both coupled cluster theory,^{31–33} second order Møller-Plesset (MP2) theory,^{34,35} and density functional theory (DFT). For the DFT calculations, the B3LYP (three parameter hybrid density functional with Becke exchange and Lee-Yang-Parr correlation; Refs. 36 and 37) and PBE0 (hybrid density functional with Perdew-Burke-Ernzerhof exchange and correlation functionals; Refs. 38 and 39) hybrid XC functionals were used. In the MP2 and DFT calculations, basis sets were employed with Gaussian exponents taken from the all-electron basis sets def2-QZVPP (valence quadruplezeta basis set with three sets of polarization functions; Ref. 40) (for H, O, F, Cl, and Br) and SARC (segmented all-electron relativistically contracted basis set; Refs. 41 and 42) (for Os, Au, Hg, Th, and U). These were re-contracted using the NESC Hamiltonian with a finite nucleus model.¹¹ For the element Hs (AN = 108), a spin-free Dirac-Hartree-Fock contracted triple-zeta basis set published by Dyall⁴³ was employed, where however, the highest contracted s, p, d, and f basis functions were replaced by 13, 10, 9, and 7 relaxed primitive functions. Then, the basis set was augmented with one f and two g sets for the purpose of improving the description of valence electron correlation and polarization. This led to a basis set of the type $(32s29p20d14f2g)/[19s15p12d9f2g]$.

Coupled cluster with single (S) and double (D) substitutions (CCSD) and coupled cluster with S and D substitutions and perturbational treatment of triple substitutions (CCSD(T)) calculations were carried out correlating all valence and semi-core electrons. For atoms F, Cl, and Br, Dyall's Dirac-contracted cc-pVTZ(pt/sf/fw) basis set⁴⁴ was employed whereas for I, the DK3-Gen-Tk/NOSeC-VTZP (Refs. 45 and 46) and for Ag and Au the cc-pwCVTZ-DK2 basis⁴⁷ was used.

TABLE I. Comparison of NESC/CCSD(T) and NESC/PBE0 dipole moments of diatomic molecules in the ground state with the corresponding experimental and other theoretical values.

Molecule	State	Method	R_e (Å)	μ (Debye)
AgF	$1\Sigma^+$	NESC/CCSD(T)	^a	6.22
		RECP/CCSD(T)/CBS (Ref. 48)	^a	6.04
		Expt. ⁵¹	1.983	6.22
AgCl	$1\Sigma^+$	NESC/CCSD(T)	^a	5.95
		RECP/CCSD(T)/CBS (Ref. 48)	^a	5.95
		Expt. ⁵¹	2.281	6.08
AgBr	$1\Sigma^+$	NESC/CCSD(T)	^a	5.74
		RECP/CCSD(T)/CBS (Ref. 48)	^a	5.67
		Expt. ⁵¹	2.393	5.62
AgI	$1\Sigma^+$	NESC/CCSD(T)	^a	5.32
		RECP/CCSD(T)/CBS (Ref. 48)	^a	5.27
		Expt. ⁵⁰		5.10
AuF	$1\Sigma^+$	NESC/CCSD(T)	^a	4.32
		RECP/CCSD(T)/CBS (Ref. 48)	^a	4.37
		Expt. ⁵²	1.918	
AuCl	$1\Sigma^+$	NESC/CCSD(T)	^a	3.81
		RECP/CCSD(T)/CBS (Ref. 48)	^a	3.90
		Expt. ⁵³	2.199	
AuBr	$1\Sigma^+$	NESC/CCSD(T)	^a	3.50
		RECP/CCSD(T)/CBS (Ref. 48)	^a	3.48
		Expt. ⁵³	2.318	
AuI	$1\Sigma^+$	NESC/CCSD(T)	^a	3.16
		RECP/CCSD(T)/CBS (Ref. 48)	^a	2.94
		Expt. ⁵³	2.506	
AuH	$1\Sigma^+$	NESC/PBE0	1.530	1.47
		RECP/MP2 (Ref. 54)	1.51	1.03
		Expt. ⁵⁵	1.524	
ThO	$1\Sigma^+$	NESC/PBE0	1.826	3.05
		RECP/CCSD(T) (Ref. 56)	1.845	2.84
		Expt. ^{57,58}	1.840	2.78
HgH	$2\Sigma^+$	NESC/PBE0	1.747	0.37
		Expt. ^{59,60}	1.741	0.47
HgF	$2\Sigma^+$	NESC/PBE0	2.039	3.69
HgCl	$2\Sigma^+$	NESC/PBE0	2.403	3.84
		Expt. ⁶¹	2.395	

^aCalculated at the experimental bond length. The NESC/CCSD(T) bond lengths for AuX are: 1.922 (X = F); 2.219 (Cl); 2.333 (Br); 2.482 Å (I).

The molecules investigated predominantly possess closed-shell character and therefore spin-orbit coupling (SOC) corrections of the electric properties do not play any significant role. In the case of the dipole moment, the largest SOC corrections were found for AgF($1\Sigma^+$) and AuI($1\Sigma^+$) (−0.10 and −0.09 Debye) (Ref. 48), whereas for X elements with smaller AN, the corrections are just fractions of these maximum values. SOC corrections become more important when fractionally occupied *p*-, *d*-, and *f*-orbitals are present. However, such molecules were not investigated in this work.

The modes of the calculated vibrational spectra were analyzed to determine their character (stretching, bending, etc.) using the composition of normal modes (CNM) analysis of Konkoli and Cremer, which is based on local vibrational modes.⁴⁹

VII. RESULTS AND DISCUSSIONS

In Tables I and II, NESC dipole moments and polarizabilities of a series of Ag-, Au-, and Hg-containing molecules

TABLE II. Polarizabilities (\AA^3) at optimized geometries as obtained with NESC/MP2, NESC/PBE0, or non-relativistic (NR) calculations. Experimental values are given in parentheses for comparison.

No.	Molecule	Method	α_{xx}	α_{yy}	α_{zz}	$\bar{\alpha}$
1	AuH	NESC/PBE0	4.99	4.99	5.45	5.14
		NESC/MP2	5.05	5.05	6.01	5.37
2	AuH ₂ ⁻	NESC/PBE0	7.29	7.29	9.73	8.11
		NESC/MP2	7.01	7.01	9.34	7.79
3	AuH ₄ ⁻	NESC/PBE0	10.01	10.01	6.42	8.81
		NESC/MP2	9.85	9.85	6.38	8.69
4	AuF	NESC/PBE0	3.96	3.96	4.78	4.24
		NESC/MP2	4.12	4.12	4.91	4.38
5	AuF ₂ ⁻	NESC/PBE0	5.40	5.40	6.36	5.72
		NESC/MP2	5.34	5.34	6.30	5.66
6	AuF ₄ ⁻	NESC/PBE0	7.07	7.07	4.36	6.17
		NESC/MP2	7.52	7.52	4.34	6.46
7	AuCl	NESC/PBE0	5.32	5.32	8.71	6.45
		NESC/MP2	5.45	5.45	9.18	6.69
8	AuCl ₂ ⁻	NESC/PBE0	7.64	7.64	14.46	9.91
		NESC/MP2	7.60	7.60	14.33	9.84
9	AuCl ₄ ⁻	NESC/PBE0	18.93	18.93	9.39	15.75
		NESC/MP2	20.19	20.19	9.32	16.57
10	AuBr	NESC/PBE0	6.01	6.01	10.56	7.53
		NESC/MP2	6.07	6.07	11.20	7.78
11	AuBr ₂ ⁻	NESC/PBE0	8.91	8.91	18.87	12.23
		NESC/MP2	8.73	8.73	18.48	11.98
12	AuBr ₄ ⁻	NESC/PBE0	25.45	25.45	11.78	20.89
		NESC/MP2	26.74	26.74	11.52	21.67
13	ThO	NESC/PBE0	22.08	22.08	16.53	20.23
		NESC/MP2	18.10	18.10	14.99	17.06
14	Th ₂ O ₂	NESC/PBE0	43.01	35.81	58.63	45.82
		NESC/MP2	34.43	30.50	47.96	37.63
15	UF ₆	NESC/PBE0	7.61	7.61	7.61	7.61
		NESC/MP2	8.03	8.03	8.03	8.03
16	OsO ₄	NESC/PBE0	6.89	6.89	6.89	6.89
		NESC/MP2	8.23	8.23	8.23	8.23 (8.17) (Ref. 51)
17	HsO ₄	NESC/PBE0	7.34	7.34	7.34	7.34
		NESC/MP2	8.30	8.30	8.30	8.30
18	HgH	NESC/PBE0	5.05	5.05	7.38	5.83
		NESC/MP2	4.56	4.56	7.27	5.46
		NR/PBE0	7.50	7.50	8.57	7.86
19	HgH ₂	NESC/PBE0	4.31	4.31	6.77	5.13
		NESC/MP2	4.19	4.19	6.66	5.01
		NR/PBE0	5.23	5.23	7.29	5.91
20	HgH ₄	NESC/PBE0	7.58	7.58	4.32	6.49
		NESC/MP2	7.55	7.55	4.28	6.46
		NR/PBE0	9.05	9.05	4.95	7.68
21	HgF	NESC/PBE0	4.37	4.37	6.53	5.09
		NESC/MP2	3.87	3.87	6.85	4.86
		NR/PBE0	6.35	6.35	6.65	6.45
22	HgF ₂	NESC/PBE0	3.31	3.31	5.75	4.13
		NESC/MP2	3.33	3.33	5.89	4.18
		NR/PBE0	3.30	3.30	5.57	4.06
23	HgF ₄	NESC/PBE0	7.35	7.35	3.39	6.03
		NESC/MP2	8.23	8.23	3.44	6.64
		NR/PBE0	8.92	8.92	3.38	7.08
24	HgCl	NESC/PBE0	5.72	5.72	10.65	7.36
		NESC/MP2	5.28	5.28	11.48	7.34 (7.4) (Ref. 51)
		NR/PBE0	7.63	7.63	10.91	8.73

TABLE II. (Continued.)

No.	Molecule	Method	α_{xx}	α_{yy}	α_{zz}	$\bar{\alpha}$
25	HgCl ₂	NESC/PBE0	6.04	6.04	13.62	8.57
		NESC/MP2	5.99	5.99	13.82	8.60
		NR/PBE0	6.39	6.39	13.16	8.65
26	HgCl ₄	NESC/PBE0	19.54	19.54	8.39	15.82
		NESC/MP2	19.32	19.32	8.38	15.68
		NR/PBE0	22.82	22.82	8.70	18.11

as well as some molecules containing Os, Th, U, or Hs are listed. For silver and gold halides, NESC/CCSD(T) dipole moments (calculated at CCSD(T) and experimental bond lengths) are close to the relativistic effective core potential (RECP)/CCSD(T)/complete basis set (CBS) dipole moments of Goll and Stoll,⁴⁸ which were obtained at the CCSD(T) level using experimental bond lengths, numerical derivatives, RECPs, and aug-cc-pVnZ ($n = 4, 5$) basis sets to extrapolate to the CBS limit. NESC/CCSD(T) reproduces the results of the latter calculations within 0.01–0.02 Debye requiring however less than 10% of the computer time needed for the RECP/CCSD(T)/CBS calculations. Both sets of calculated dipole moments predict the experimental values with an accuracy of 0.2 Debye or better. For example, the NESC/CCSD(T) dipole moment of AgI (5.32 Debye) supports an earlier measured value of 5.10 Debye⁵⁰ rather than the value of 4.55 Debye listed in the Handbook of Chemistry and Physics.⁵¹ It is interesting to note that the corresponding NESC/CCSD dipole moments are about 0.3 Debye larger than NESC/CCSD(T) values.

The calculation of the isotropic polarizability of osmium tetroxide, OsO₄, and hassium tetroxide, HsO₄, were performed to compare calculated polarizabilities with experimental or previously published values. The data in Table II reveal that the NESC/MP2 value of the isotropic polarizability (8.23 \AA^3) is in close agreement with the experimental value of 8.17 \AA^3 and somewhat better than the IORAmM/MP2 value obtained previously (8.38 \AA^3).²⁸ NESC/MP2 also predicts that the isotropic polarizability of HsO₄ is somewhat larger (8.30 \AA^3 , Table II) than that of OsO₄ in contradiction to the IORAmM/MP2 result,²⁸ however in agreement with the expectation that with increasing number of electrons and a more electropositive central atom, the polarizability increases rather than decreases. The NESC/PBE0 results for $\bar{\alpha}$ of the group VIII tetroxides are more than 1 unit too small (6.89 \AA^3). In general, NESC/MP2 polarizabilities are more reliable than the NESC/PBE0 results for $\bar{\alpha}$, which means that DFT can only be used for considering general trends. However, there are also cases (see, e.g., the NESC/PBE0 value for HgCl in Table II) where the NESC/DFT result agrees well with measured polarizabilities.

For some of the molecular polarizabilities listed in Table II, we have added the non-relativistic electric properties obtained with the same DFT method and basis set. Relativistic corrections for the dipole moments are between -0.2 and -0.7 Debye (HgH: 0.37–1.03 = -0.66 Debye; HgF: 3.69–4.05 = -0.36 Debye) and for the isotropic

TABLE III. Comparison of NESC geometries (distances in Å), vibrational frequencies (cm⁻¹), and infrared intensities scaled by the degeneracies (km/mol) with the corresponding experimental values measured in the gas or the solid phase (the latter is indicated by *solid*).

No.	Mol. (Sym.)	Method	Geometry	Frequency (infrared intensity, mode symmetry)
1	AuH (<i>C_{∞v}</i>)	NESC/PBE0 Expt. ⁵⁵	Au-H: 1.530 Au-H: 1.524	2283.7 (14.7; σ ⁺) 2305.0 (σ ⁺)
2	AuH ₂ ⁻ (<i>D_{∞h}</i>)	NESC/PBE0 Expt. ⁶³	Au-H: 1.652	773.8 (115.7; π _u), 1685.2 (1035.8; σ _u ⁺), 1994.9 (0; σ _g ⁺) 1636.0 (σ _u ⁺)
3	AuH ₄ ⁻ (<i>D_{4h}</i>)	NESC/PBE0 Expt. ⁶³	Au-H: 1.631	776.4 (0; b _{2g}), 793.9 (66.6; e _u), 828.7 (42.3; a _{2u}), 843.1 (0; b _{2u}), 1780.6 (2318.0; e _u), 2113.7 (0; b _{1g}), 2118.1 (0; a _{1g}) 1676.4 (e _u)
4	AuF (<i>C_{∞v}</i>)	NESC/PBE0 Expt. ⁵²	Au-F: 1.923 Au-F: 1.918	556.7 (52.3; σ ⁺) 563.7 (σ ⁺)
5	AuF ₂ ⁻ (<i>D_{∞h}</i>)	NESC/PBE0	Au-F: 1.963	184.4 (25.0; π _u), 516.3 (0; σ _g ⁺), 548.1 (182.7; σ _u ⁺)
6	AuF ₄ ⁻ (<i>D_{4h}</i>)	NESC/PBE0 Expt.(solid) ⁶⁴	Au-F: 1.916	184.0 (0; b _{2u}), 217.7 (0; b _{2g}), 233.1 (25.8; a _{2u}), 253.8 (8.7; e _u), 572.0 (0; b _{1g}), 597.1 (0; a _{1g}), 613.4 (383.9; e _u) 230 (b _{2g}), 561 (b _{1g}), 588 (a _{1g})
7	AuCl (<i>C_{∞v}</i>)	NESC/PBE0 Expt. ⁵³	Au-Cl: 2.209 Au-Cl: 2.199	375.2 (12.9; σ ⁺) 383.6 (σ ⁺)
8	AuCl ₂ ⁻ (<i>D_{∞h}</i>)	NESC/PBE0 Expt.(solid) ^{65,66}	Au-Cl: 2.275 Au-Cl: 2.28	106.4 (16.8; π _u), 322.2 (0; σ _g ⁺), 342.6 (70.5; σ _u ⁺) 112/120 (π _u), 329 (σ _g ⁺), 350 (σ _u ⁺)
9	AuCl ₄ ⁻ (<i>D_{4h}</i>)	NESC/PBE0 Expt.(solid) ⁶⁶	Au-Cl: 2.290	83.0 (0; b _{2u}), 139.5 (8.6; a _{2u}), 159.0 (0; b _{2g}), 159.8 (0.0; e _u), 321.3 (0; b _{1g}), 345.6 (0; a _{1g}), 355.0 (161.0; e _u) 171 (b _{2g}), 179 (e _u), 324 (b _{1g}), 347 (a _{1g}), 350 (e _u)
10	AuBr (<i>C_{∞v}</i>)	NESC/PBE0 Expt. ⁵³	Au-Br: 2.332 Au-Br: 2.318	257.8 (5.1; σ ⁺) 264.4 (σ ⁺)
11	AuBr ₂ ⁻ (<i>D_{∞h}</i>)	NESC/PBE0 Expt.(solid) ^{65,66}	Au-Br: 2.403 Au-Br: 2.40	71.4 (5.9; π _u), 201.3 (0; σ _g ⁺), 246.7 (34.6; σ _u ⁺) 75/79 (π _u), 209 (σ _g ⁺), 254 (σ _u ⁺)
12	AuBr ₄ ⁻ (<i>D_{4h}</i>)	NESC/PBE0 Expt.(solid) ⁶⁶	Au-Br: 2.437	45.2 (0; b _{2u}), 98.9 (0; b _{2g}), 100.0 (2.5; a _{2u}), 102.1 (1.1; e _u), 193.4 (0; b _{1g}), 210.7 (0; a _{1g}), 249.5 (73.6; e _u) 102 (b _{2g}), 110 (e _u), 196 (b _{1g}), 212 (a _{1g}), 252 (e _u)
13	ThO (<i>C_{∞v}</i>)	NESC/PBE0 Expt. ⁵⁷	Th-O: 1.826 Th-O: 1.840	926.1 (245.7; σ ⁺) 895.8 (σ ⁺)
14	Th ₂ O ₂ (<i>D_{2h}</i>)	NESC/PBE0 Expt. ⁶⁷	Th-O: 2.089 O-Th-O: 74.4	155.7 (4.8; b _{3u}), 192.7 (0; a _g), 373.1 (0; b _{3g}), 527.2 (35.2; b _{2u}), 623.8 (297.9; b _{1u}), 633.9 (0; a _g) 619.7 (b _{1u})
15	UF ₆ (<i>O_h</i>)	NESC/PBE0 Expt. ^{68,69}	U-F: 1.994 U-F: 1.996	139.1 (0; t _{2u}), 184.0 (51.7; t _{1u}), 199.3 (0; t _{2g}), 539.1 (0; e _g), 629.4 (810.3; t _{1u}), 681.4 (0; a _{1g}) 142 (t _{2u}), 186.2 (~38; t _{1u}), 202 (t _{2g}), 532.5 (e _g), 624 (750; t _{1u}), 667.1 (a _{1g})
16	OsO ₄ (<i>T_d</i>)	NESC/PBE0 Expt. ^{70,71}	Os-O: 1.686 Os-O: 1.711	352.6 (22.4; t ₂), 356.5 (0; e), 1031.9 (465.8; t ₂), 1063.9 (0; a ₁) 322.7 (t ₂), 333.1 (e), 960.1 (t ₂), 965.2 (a ₁)
17	²⁶⁵ HsO ₄ (<i>T_d</i>)	NESC/PBE0	Hs-O: 1.757	316.1 (32.9; t ₂), 335.2 (0; e), 1010.4 (463.2; t ₂), 1056.2 (0; a ₁)

polarizabilities between -0.2 and -2.0 \AA^3 where the largest effects are found for HgH ($\bar{\alpha}$: $5.83-7.86 = -2.03 \text{ \AA}^3$). These trends can be related to the relativistic orbital contraction of the $6s$ -orbital of Hg, which dominates scalar relativistic effects of mercury compounds. The exception is found for HgF₂ where the effect of the $6s$ -orbital contraction is balanced by the electron-withdrawing ability of two strongly electronegative F atoms so that relativistic and non-relativistic isotropic polarizability (4.13 and 4.06 \AA^3 , Table II) become comparable.

The relativistic dipole moments and polarizabilities follow well-known trends. The dipole moments increase with increasing bond length and increasing bond polarity (i.e., electronegativity difference of the atoms being bonded) where the latter effect dominates as can be seen in the series AuX with X = H, F, Cl, Br, I ($1.47, 4.32, 3.81, 3.50, 3.16$ Debye; Table I). The polarizability is a volume property and therefore increases with the size of the molecule and the number of

electrons (see, e.g., AuX with X = F, Cl, Br: $\bar{\alpha} = 4.38, 6.69, 7.78 \text{ \AA}^3$). Isotropic polarizabilities of anions are larger than those of neutral molecules (see, e.g., HgCl₂ and AuCl₂⁻: 8.60 and 9.84 \AA^3) and cations, those of radicals larger than those of closed shell systems (see, e.g., HgH and HgH₂: 5.46 and 5.01 \AA^3). Also, molecules with more electropositive atoms possess a larger isotropic polarizability than molecules with more electronegative atoms (see, e.g., HgH and HgF: 5.46 vs. 4.86 \AA^3). All these trends are reflected by the NESC polarizabilities of the molecules listed in Table II.

As in the case of the dipole moments, the NESC polarizabilities help to correct flawed experimental data. For example, the measured isotropic polarizability of UF₆ is given to be 12.5 \AA^3 ,⁶² which is far too large in view of a NESC/MP2 value of 8.03 \AA^3 . The latter value is in line with RECP/CCSD, RECP/DFT, ZORA (zero order regular approximation)/DFT, and SOC-ZORA (ZORA with spinorbit coupling)/DFT results obtained in

TABLE IV. Comparison of NESC/B3LYP frequencies of $\text{UO}_2(\text{NO}_3)_2 \cdot 2 \text{DMF}$ (C_2 -symmetry) with experimental values. The infrared intensities of infrared active vibrational modes are given in the parentheses.

Sym	Method	Frequency (cm^{-1})
a	NESC/B3LYP	12 (5), 25, 41 (3), 100 (2), 103, 130, 132, 162 (2), 179 (1), 256, 365, 373 (30), 406, 688, 715, 759, 828 (13), 869, 889, 968 (354; O-U-O anti-stretch), 1050, 1067, 1079, 1126, 1132 (1), 1182 (4), 1269, 1294, 1417, 1450, 1456, 1475, 1483 (8), 1504, 1505 (32), 1547, 1597, 1708, 3028, 3035, 3080 (47), 3080, 3087 (21), 3131, 3162
	Expt. ⁷⁴	929
b	NESC/B3LYP	20, 35 (3), 38, 56, 87, 91, 92 (22), 127, 141 (8), 154 (7), 156, 172, 205, 210, 212 (7), 213, 213, 216 (33), 252 (79; O-U-O bend), 258, 264 (132; O-U-O bend), 364 (69; C-N-C bend), 373, 406 (15), 685 (127; DMF breath), 713 (2), 755 (62; O-N-O bend), 828, 869 (4), 1050, 1066 (86; N-O stretch), 1079 (22), 1125 (263; DMF twist), 1132, 1182, 1269 (56), 1301 (739; N-O anti-stretch), 1416 (205; DMF twist), 1450 (20), 1455 (32), 1475 (97; DMF twist), 1483, 1504 (13), 1505, 1546 (50), 1588 (1498; N-O stretch), 1693 (2109; C-O stretch), 3028 (56), 3034 (105; C-H stretch), 3080, 3080 (62), 3087, 3131 (15), 3162 (3)
	Expt. ⁷⁴	1283, 1524, 1648

this work (variation by $\pm 0.5 \text{ \AA}^3$). The same is true in the case of $\bar{\alpha}(\text{HgCl}_2)$, which is given in the literature⁶² as 11.6 \AA^3 whereas the calculated NESC/MP2 value is 8.60 \AA^3 .

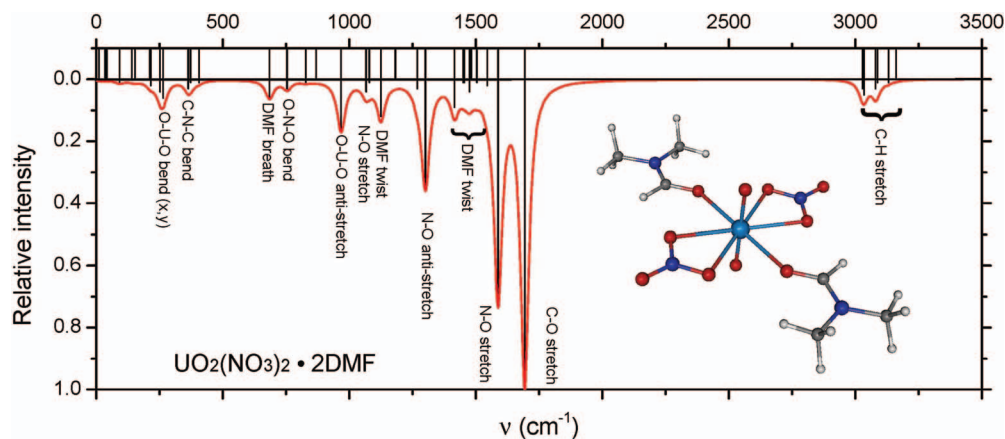
In Table III, NESC/PBE0 geometries, vibrational frequencies, and IR intensities are compared with experimental results, some of which were obtained in the solid state (as indicated). Previously, Schwerdtfeger and co-workers investigated some of the Au-containing molecules at lower levels of theory using RECPs.^{72,73} Calculated vibrational frequencies are in reasonable agreement with the available experimental data considering (i) the harmonic approximation and (ii) the fact that NESC/PBE0 gives the calculated bond lengths somewhat too long. In general, stretching frequencies are somewhat too large (due to the harmonic approximation) whereas bending frequencies are somewhat too small (due to the somewhat too long bond lengths). In such a situation, it is difficult to find a common scaling value. Future work has to focus on the calculation of NESC anharmonicity corrections.

Although many vibrational spectra have been measured, there is a serious lack of measured absolute IR intensities. Only in the case of UF_6 , experimental absolute intensities are available.⁶⁹ Both theory and experiment agree that the t_{1u} -symmetrical modes at 184 (exp.: 186) and 629 (exp.: 624) cm^{-1} with intensities of 52 (exp.: 38) and 810 (exp.: 750)

km/mol can be used to identify the molecule in the gas phase. The good agreement with the experimental values confirms that the methods developed are capable of yielding reliable IR intensities.

IR intensities reflect changes in the bond polarity (bond dipole moment) during the vibration. In a simplified way, intensities become larger as the partner atom becomes more electronegative. For example, in the series AuX with $X = \text{Br}, \text{Cl}, \text{F}$, the intensity of the stretching mode increases from 5.1 to 12.9 and 52.3 km/mol (NESC/PBE0; Table III). The intensity increases in the corresponding anions XAuX^- : 35, 70, 183 km/mol (σ_u^+ -stretching mode) and 6, 17, 25 km/mol (π_u -bending mode). It is known that IR-intensities can be used to derive effective atomic charges provided the charge flux during a vibrational motion is available from another source.²⁰

In Table IV, the NESC/B3LYP frequencies and intensities of $\text{UO}_2(\text{NO}_3)_2 \cdot 2 \text{DMF}$ (dimethylformamide) are given for the gas phase. This compound was recently investigated in the solid state where it turned out difficult to measure exact IR intensities.⁷⁴ In Figure 1, the calculated spectrum is shown, which reveals that the vibrational modes involving the uranium atom appear at 968 cm^{-1} (antisymmetric O-U-O stretch) and in the far-IR (the O-U-O bending modes, denoted as (x,y), at 252 and 264 cm^{-1}). Since the stretching mode has a larger intensity, it is better suited for identification of the compound.

FIG. 1. NESC/B3LYP infrared spectrum of $\text{UO}_2(\text{NO}_3)_2 \cdot 2 \text{DMF}$ in the gas phase.

VIII. CONCLUSIONS

In this work, we have extended the applicability possibilities of the NESC method:

(1) We have developed the methodology for routinely calculating electric second order response properties with the help of analytic second energy derivatives of the NESC method with regard to the components of an external electric field.

(2) We have presented the methodology needed for the calculation of the static dipole polarizability and the IR intensity where suitable working formulas have been tested.

(3) In this connection, we have also checked NESC dipole moments. A comparison of NESC/CCSD(T) dipole moments for AgX and AuX diatomic closed shell molecules has found them as accurate as the much more expensive RECP/CCSD(T)/CBS dipole moments.

(4) NESC/MP2 polarizabilities correctly reflect their dependence on the volume of the molecule, the molecular charge, the spin multiplicity, and the electronegativity of the atoms forming the molecule. NESC/PBE0 polarizabilities are less accurate, however they are sufficiently accurate to predict general trends.

(5) NESC/MP2 isotropic polarizabilities compare well with the corresponding experimental values as, e.g., in the case of OsO₄. They predict a larger polarizability for HsO₄ and reveal that the experimental values for UF₆ and HgCl₂ are erroneous.

(5) The calculated NESC/PBE0 frequencies and IR intensities agree very well with the available experimental data for UF₆. NESC/PBE0 IR intensities are in line with the known charge distributions, dipole moments, and the dependence of the latter on geometrical changes.

In summary, we have proven that analytic NESC second derivative calculations can routinely be carried out and that in this way, NESC electric second order response properties become generally available. The applicability range and the usefulness of NESC have been substantially increased in this way. The methodology presented in this work is also of relevance for other exact two-component relativistic methods such as the IOTC (infinite order two component) or X2C (exact two component) method.

ACKNOWLEDGMENTS

This work was financially supported by the National Science Foundation (Grant No. CHE 1152357). We thank the SMU for providing computational resources.

- ¹Y. Yamaguchi, J. D. Goddard, Y. Osamura, and H. F. S. Schaefer, *A New Dimension to Quantum Chemistry: Analytic Derivative Methods in Ab Initio Molecular Electronic Structure Theory* (Oxford University Press, Oxford, 1994).
- ²C. E. Dykstra, S.-J. Liu, and D. J. Malik, in *Advances in Chemical Physics*, edited by I. Prigogine, and S. Rice (Wiley, New York, 1989), Vol. 75, pp. 37–111.
- ³K. G. Dyall and K. Fægri, *Introduction to Relativistic Quantum Chemistry* (Oxford University Press, Oxford, 2007).
- ⁴T. Saue, *Chem. Phys. Chem.* **12**, 3077 (2011).
- ⁵D. Peng and M. Reiher, *Theor. Chem. Acc.* **131**, 1081 (2012).
- ⁶L. Visscher, T. Saue, and J. Oddershede, *Chem. Phys. Lett.* **274**, 181 (1997).
- ⁷P. Norman, B. Schimmelpfennig, K. Ruud, H. J. A. Jensen, and H. Ågren, *J. Chem. Phys.* **116**, 6914 (2002).

- ⁸M. Pecul and A. Rizzo, *Chem. Phys. Lett.* **370**, 578 (2003).
- ⁹P. Schwerdtfeger, "The ctc table of experimental and calculated static dipole polarizabilities for the electronic ground states of the neutral elements," (2012). See <http://ctcp.massey.ac.nz/dipole-polarizabilities> and references cited therein.
- ¹⁰K. G. Dyall, *J. Chem. Phys.* **106**, 9618 (1997).
- ¹¹W. Zou, M. Filatov, and D. Cremer, *Theor. Chem. Acc.* **130**, 633 (2011).
- ¹²W. Zou, M. Filatov, and D. Cremer, *J. Chem. Phys.* **134**, 244117 (2011).
- ¹³M. Filatov, W. Zou, and D. Cremer, *J. Phys. Chem. A* **116**, 3481 (2012).
- ¹⁴M. Filatov, W. Zou, and D. Cremer, *J. Chem. Theory Comput.* **8**, 875 (2012).
- ¹⁵M. Filatov, W. Zou, and D. Cremer, *J. Chem. Phys.* **137**, 054113 (2012).
- ¹⁶W. Zou, M. Filatov, and D. Cremer, *J. Chem. Theory Comput.* **8**, 2617 (2012).
- ¹⁷C. J. E. Boettcher, *Theory of Electric Polarization* (Elsevier, Amsterdam, 1973).
- ¹⁸V. Kellö, A. Antušek, and M. Urban, *J. Comput. Methods Sci. Eng.* **4**, 753 (2004).
- ¹⁹G. Zerbi, in *Vibrational Intensities in Infrared and Raman Spectroscopy*, edited by W. Person, and G. Zerbi (Elsevier, Amsterdam, 1982), p. 23.
- ²⁰D. Cremer, J. A. Larsson, and E. Kraka, in *Theoretical and Computational Chemistry, Theoretical Organic Chemistry*, Vol. 5, edited by C. Parkanyi (Elsevier, Amsterdam, 1998), p. 259.
- ²¹P. A. M. Dirac, *Proc. R. Soc. London A* **117**, 610 (1928).
- ²²P. A. M. Dirac, *Proc. R. Soc. London A* **123**, 714 (1929).
- ²³M. Filatov and D. Cremer, *J. Chem. Phys.* **122**, 064104 (2005).
- ²⁴M. Filatov, *J. Chem. Phys.* **125**, 107101 (2006).
- ²⁵M. Filatov and K. G. Dyall, *Theor. Chem. Acc.* **117**, 333 (2007).
- ²⁶K. G. Dyall, *J. Comp. Chem.* **23**, 786 (2002).
- ²⁷W. Liu and D. Peng, *J. Chem. Phys.* **131**, 031104 (2009).
- ²⁸M. Filatov and D. Cremer, *J. Chem. Phys.* **119**, 1412 (2003).
- ²⁹E. Kraka, M. Filatov, W. Zou, J. Gräfenstein, D. Izotov, J. Gauss, Y. He, A. Wu, V. Polo, L. Olsson, Z. Konkoli, Z. He, and D. Cremer, COLOGNE2012 (Southern Methodist University, Dallas, USA, 2012).
- ³⁰M. Filatov and D. Cremer, *J. Chem. Phys.* **118**, 6741 (2003).
- ³¹G. D. Purvis III and R. J. Bartlett, *J. Chem. Phys.* **76**, 1910 (1982).
- ³²K. Raghavachari, G. W. Trucks, J. A. Pople, and M. Head-Gordon, *Chem. Phys. Lett.* **157**, 479 (1989).
- ³³T. D. Crawford and H. F. Schaefer, *Rev. Comput. Chem.* **14**, 33 (2000).
- ³⁴D. Cremer, in *Encyclopedia of Computational Chemistry*, edited by P. V. R. Schleyer, N. L. Allinger, T. Clark, J. Gasteiger, P. A. Kollman, H. F. Schaefer, and P. R. Schreiner (Wiley, Chichester, 1998), Vol. 3, p. 1706.
- ³⁵D. Cremer, in *Wiley Interdisciplinary Reviews: Computational Molecular Science*, edited by P. R. Schreiner, and W. Allen (Wiley, New York, 2011), Vol. 1, pp. 509–530.
- ³⁶A. D. Becke, *J. Chem. Phys.* **98**, 5648 (1993).
- ³⁷P. J. Stevens, F. J. Devlin, C. F. Chablowski, and M. J. Frisch, *J. Phys. Chem.* **98**, 11623 (1994).
- ³⁸J. P. Perdew, K. Burke, and M. Ernzerhof, *Phys. Rev. Lett.* **77**, 3865 (1996).
- ³⁹C. Adamo and V. Barone, *J. Chem. Phys.* **110**, 6158 (1998).
- ⁴⁰F. Weigend and R. Ahlrichs, *Phys. Chem. Chem. Phys.* **7**, 3297 (2005).
- ⁴¹D. A. Pantazis, X.-Y. Chen, C. R. Landis, and F. Neese, *J. Chem. Theory Comput.* **4**, 908 (2008).
- ⁴²D. A. Pantazis and F. Neese, *J. Chem. Theory Comput.* **7**, 677 (2011).
- ⁴³K. G. Dyall, *Theor. Chem. Acc.* **129**, 603 (2011).
- ⁴⁴See <https://bse.pnl.gov/bse/portal> for more information on EMSL basis set exchange.
- ⁴⁵H. Tatewaki and T. Koga, *Chem. Phys. Lett.* **328**, 473 (2000).
- ⁴⁶See <http://setani.sci.hokudai.ac.jp/sapporo/Welcome.do> for more information on data base of segmented gaussian basis sets, Quantum Chemistry Group, Sapporo, Japan.
- ⁴⁷K. A. Peterson and C. Pizzarini, *Theor. Chem. Acc.* **114**, 283 (2005).
- ⁴⁸E. Goll, H. Stoll, C. Tierfelder, and P. Schwerdtfeger, *Phys. Rev. A* **76**, 032507 (2007).
- ⁴⁹Z. Konkoli and D. Cremer, *Int. J. Quantum Chem.* **67**, 29 (1998).
- ⁵⁰J. Hoefst and K. P. R. Nair, *J. Mol. Struct.* **97**, 347 (1983).
- ⁵¹D. R. Lide, *CRC Handbook of Chemistry and Physics*, 90th ed. (CRC, Boca Raton, FL, 2009).
- ⁵²T. Okabayashi, Y. Nakaoka, E. Yamazaki, and M. Tanimoto, *Chem. Phys. Lett.* **366**, 406 (2002).
- ⁵³L. M. Reynard, C. J. Evans, and M. C. L. Gerry, *J. Mol. Spectrosc.* **205**, 344 (2001).
- ⁵⁴P. Pykkö, X.-G. Xiong, and J. Li, *Faraday Discuss.* **152**, 169 (2011).

- ⁵⁵K. P. Huber and G. Herzberg, *Molecular Spectra and Molecular Structure IV. Constants of Diatomic Molecules* (Van Nostrand Reinhold, New York, 1979).
- ⁵⁶A. A. Buchachenko, *J. Chem. Phys.* **133**, 041102 (2010).
- ⁵⁷V. Goncharov and M. C. Heaven, *J. Chem. Phys.* **124**, 064312 (2006).
- ⁵⁸F. Wang, A. Le, T. C. Steimle, and M. C. Heaven, *J. Chem. Phys.* **134**, 031102 (2011).
- ⁵⁹J. Dufayard, B. Majourat, and O. Nedelec, *Chem. Phys.* **128**, 537 (1988).
- ⁶⁰O. Nedelec, B. Majourat, and J. Dufayard, *Chem. Phys.* **134**, 137 (1989).
- ⁶¹A. K. Rai, S. B. Rai, and D. K. Rai, *J. Phys. B* **15**, 3239 (1982).
- ⁶²A. A. Maryott and F. Buckley, U. S. National Bureau of Standards, Circular N. 537 (1953).
- ⁶³L. Andrews and X. Wang, *J. Am. Chem. Soc.* **125**, 11751 (2003).
- ⁶⁴K. Leary and N. Bartlett, *J. Chem. Soc., Chem. Commun.* **1972**, 903.
- ⁶⁵S. Mishra, V. Vallet, and W. Domcke, *Chem. Phys. Chem.* **7**, 723 (2006).
- ⁶⁶K. Nakamoto, *Infrared and Raman Spectra of Inorganic and Coordination Compounds*, 4th ed. (Wiley, New York, 1986).
- ⁶⁷L. Andrews, Y. Gong, B. Liang, V. E. Jackson, R. Flamerich, S. Li, and D. A. Dixon, *J. Phys. Chem. A* **115**, 14407 (2011).
- ⁶⁸H. H. Claassen, G. L. Goodman, J. H. Holloway, and H. Selig, *J. Chem. Phys.* **53**, 341 (1970).
- ⁶⁹W. B. Person, K. C. Kim, G. M. Campbell, and H. J. Dewey, *J. Chem. Phys.* **85**, 5524 (1986).
- ⁷⁰B. Krebs and K.-D. Hasse, *Acta Crystallogr. B* **32**, 1334 (1976).
- ⁷¹J. L. Huston and H. H. Claassen, *J. Chem. Phys.* **52**, 5646 (1970).
- ⁷²P. Schwerdtfeger, P. D. W. Boyd, A. K. Burrell, and W. T. Robinson, *Inorg. Chem.* **29**, 3593 (1990).
- ⁷³P. Schwerdtfeger, P. D. W. Boyd, S. Brienne, and A. K. Burrell, *Inorg. Chem.* **31**, 3411 (1992).
- ⁷⁴A. Prestianni, L. Joubert, A. Chagnes, G. Cote, M.-N. Ohnet, C. Rabbe, M.-C. Charbonnel, and C. Adamo, *J. Phys. Chem. A* **114**, 10878 (2010).